SUPPLEMENTARY INFORMATION

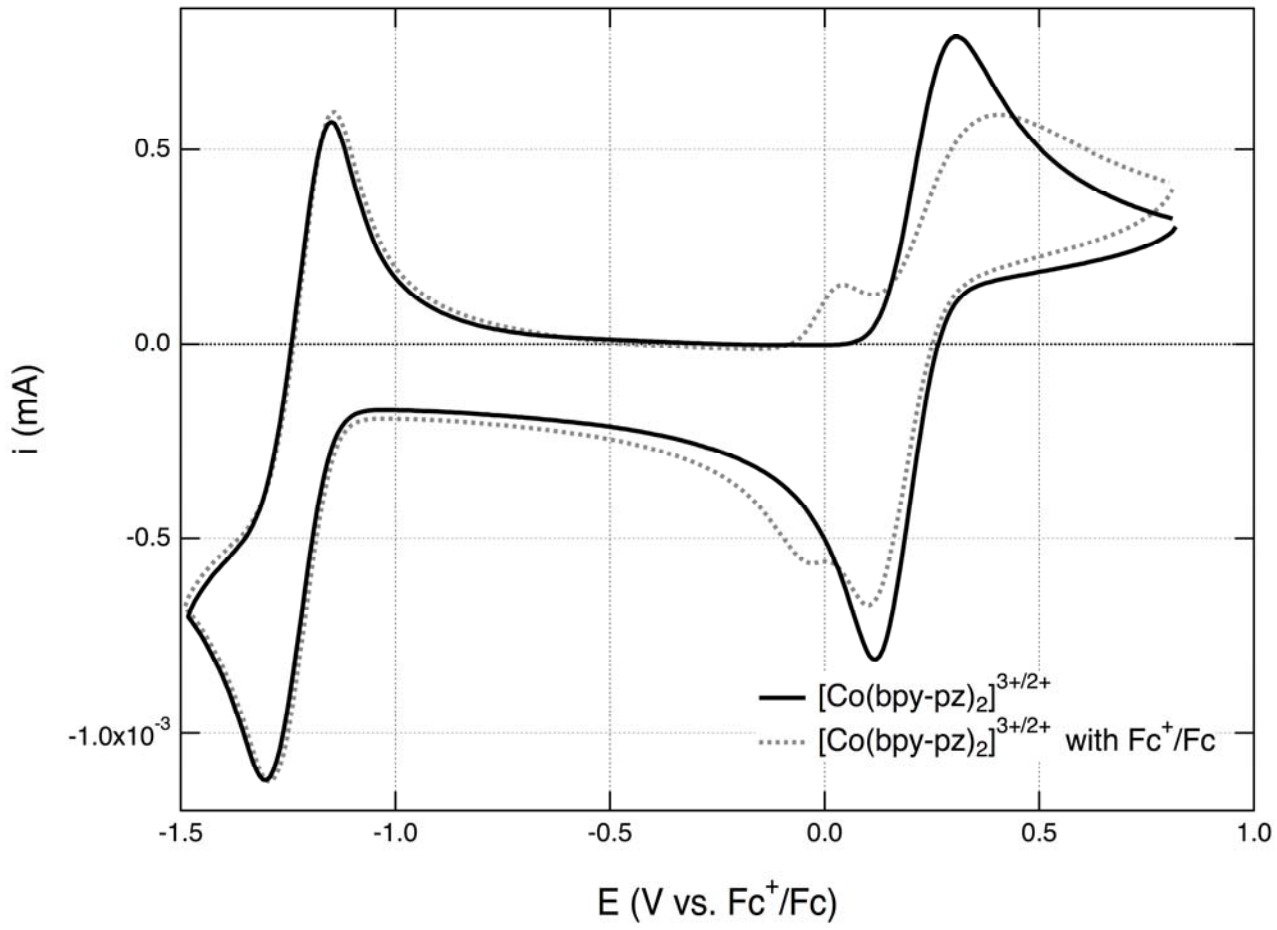

Supplementary Figure S1. Cyclic voltammetry of the $[Co(bpy\text{-}pz)_2]^{2+}$ complex. Cyclic voltammetry experiments measured using 2 mM solution of $[Co(bpy\text{-}pz)_2]^{2+}$ in acetonitrile with 0.1 M tetrabutylammonium hexafluorophosphate ($TBAPF_6$) electrolyte with Pt deposited on FTO (0.7 cm^2), a Pt plate and a Pt wire used as working, counter and reference electrode, respectively.

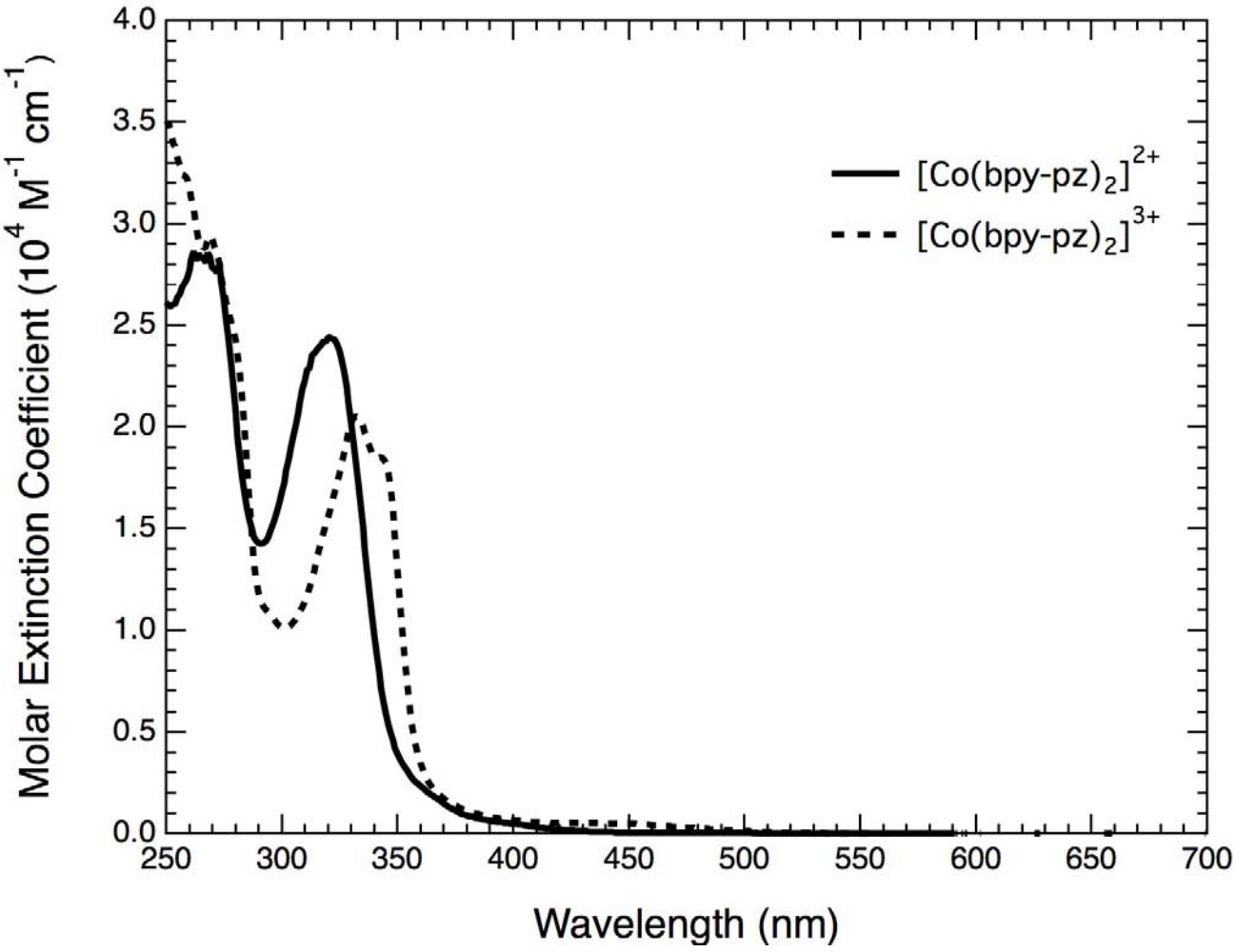

Supplementary Figure S2. UV-Vis absorption spectra of cobalt complexes. The solid line show absorption properties of the reduced state of the cobalt complex $[Co(bpy\text{-}pz)_2]^{2+}$ and the dashed line is oxidized state of the cobalt complex $[Co(bpy\text{-}pz)_2]^{3+}$ measured by dissolving in acetonitrile solution.

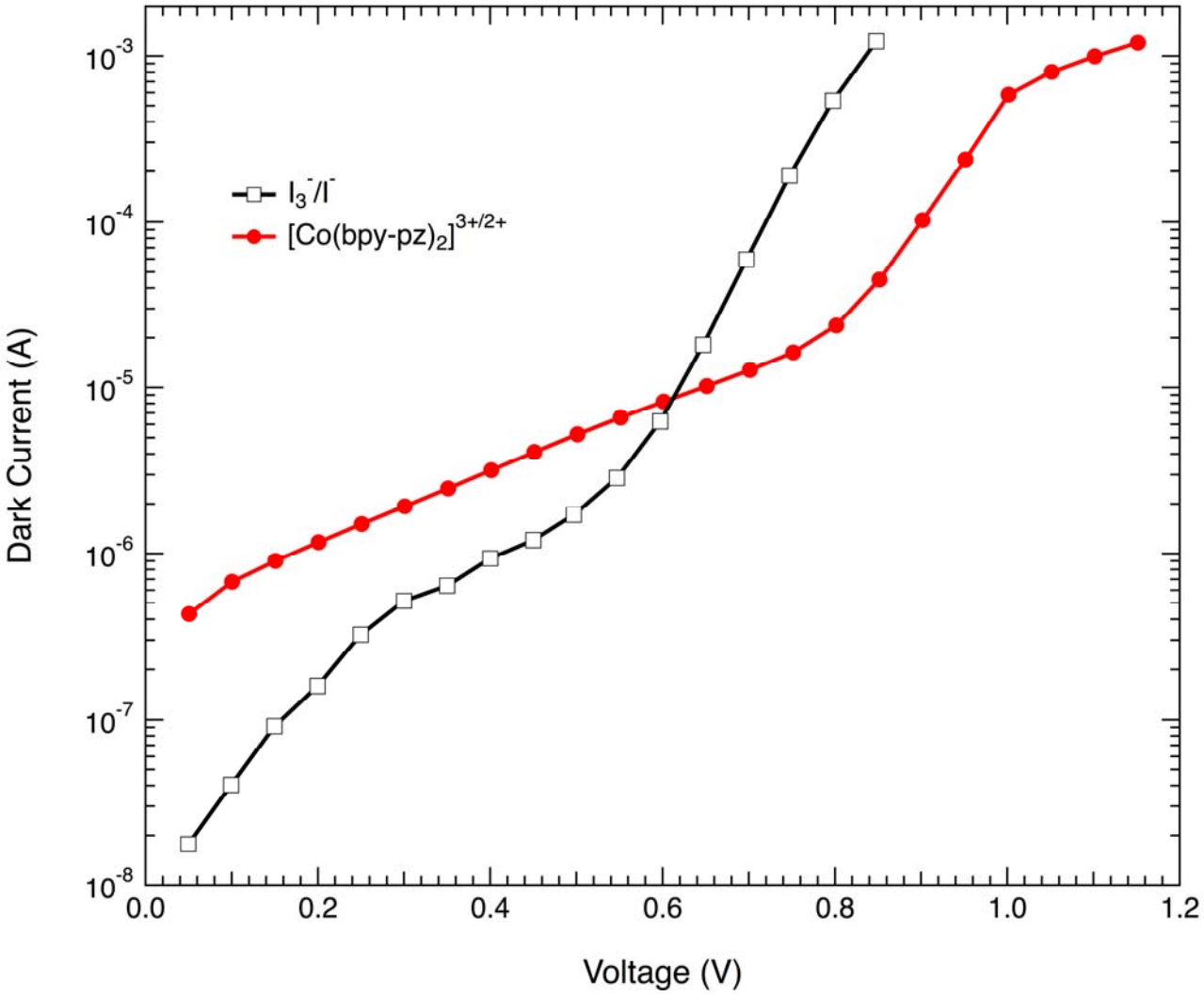

Supplementary Figure S3. Dark currents of the redox systems. Comparison of the I_3^-/I^- and $[Co(bpy\text{-}pz)_2]^{3+/2+}$ redox systems dark current near 0 V measured by the EIS.

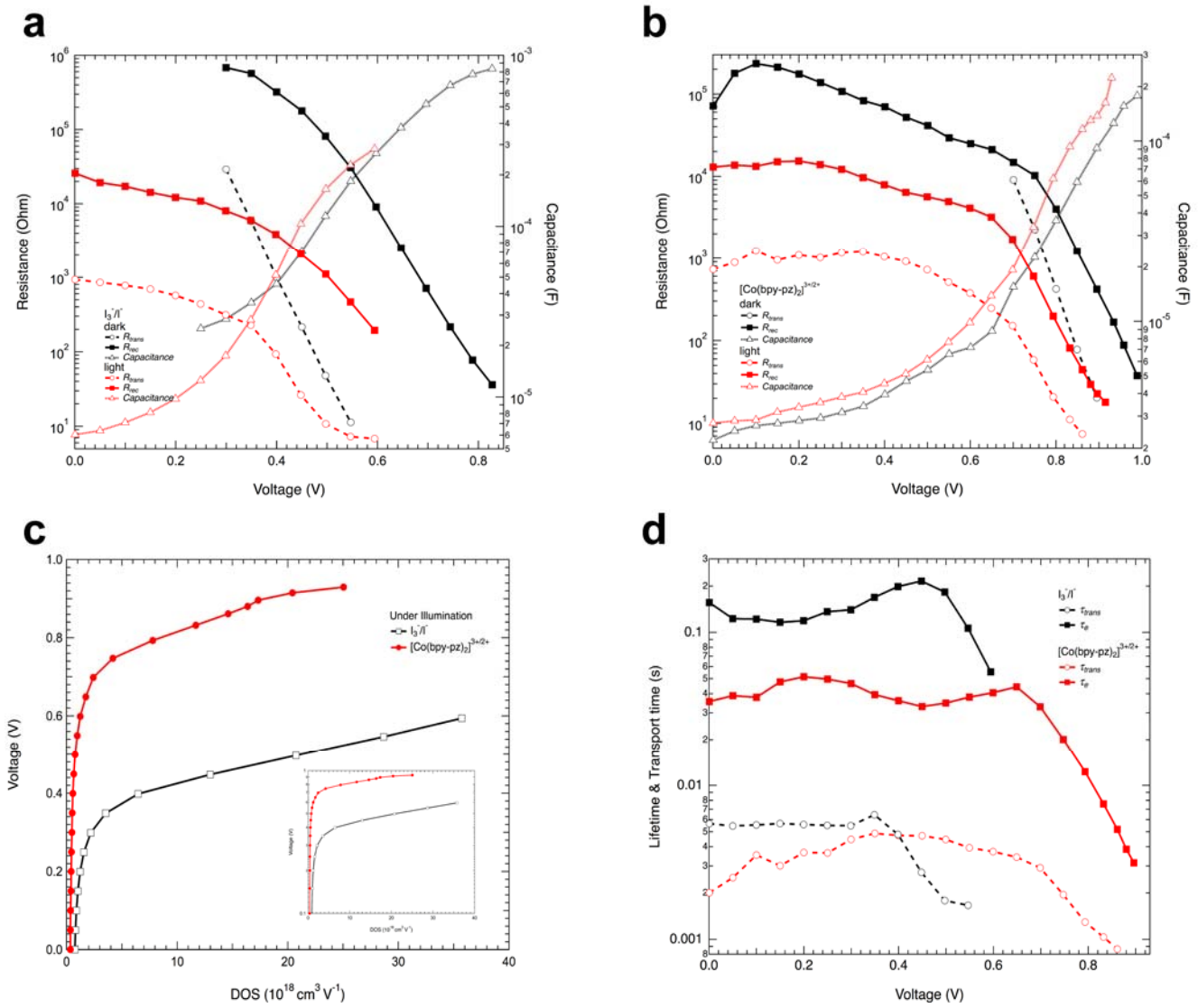

Supplementary Figure S4. EIS results of I_3^-/I^- and $[Co(bpy\text{-}pz)_2]^{3+/2+}$ system. (a) Transport resistance (R_{trans}), recombination resistance (R_{rec}), chemical capacitance, and charge transfer resistance (R_{CT}) of I_3^-/I^--based DSCs at dark (black lines) and 1 sun (red lines). (b) Transport resistance (R_{trans}), recombination resistance (R_{rec}), chemical capacitance, and charge transfer resistance (R_{CT}) of $[Co(bpy\text{-}pz)_2]^{3+/2+}$-based DSCs at dark (black lines) and 1 sun (red lines). (c) Density of states (DOS) as function of potential of the $[Co(bpy\text{-}pz)_2]^{3+/2+}$ (red lines and closed circles) and I_3^-/I^- (black lines and open squares) system based DSC under illumination (insert with a logarithmic scale). (d) Electron lifetime (solid lines with closed squares) and transport time (dashed lines with open circles) of I_3^-/I^--based (black lines) and $[Co(bpy\text{-}pz)_2]^{3+/2+}$-based (red lines) DSCs as function of bias voltage.

Supplementary Table S1. *J-V* characterization data of the DSCs. The short circuit current, open circuit potential and fill factor data were obtained employing $[Co(bpy\text{-}pz)_2]^{3+/2+}$ and I_3^-/I^- redox systems with 5.6 μm thin thick TiO_2 films under different incident light intensity conditions.

Redox	I_0 (mW cm^{-2})	J_{sc} (mA cm^{-2})	V_{oc} (mV)	FF (%)	η (%)
$[Co(bpy\text{-}pz)_2]^{3+/2+}$	100	12.33 ± 0.31	1016 ± 4	69.3 ± 0.4	8.66 ± 0.19
	51	6.50 ± 0.10	995 ± 3	74.0 ± 0.7	9.38 ± 0.22
	9.5	1.23 ± 0.02	935 ± 6	77.0 ± 1.8	9.35 ± 0.40
I^-/I_3^-	100	13.01 ± 0.23	745 ± 12	66.5 ± 0.3	6.45 ± 0.14
	51	6.70 ± 0.10	734 ± 9	70.0 ± 0.1	6.80 ± 0.05
	9.5	1.29 ± 0.15	703 ± 10	73.7 ± 0.1	7.01 ± 0.02

Supplementary Table S2. *J-V* characterization data of the DSCs. The short circuit current, open circuit potential and fill factor data were obtained employing $[Co(bpy\text{-}pz)_2]^{3+/2+}$ with various TiO_2 film thickness under different incident light intensity conditions.

TiO_2 (μm)	I_0 (mW cm^{-2})	J_{sc} (mA cm^{-2})	V_{oc} (mV)	*FF* (%)	η (%)
2.8	100	10.84 ± 0.13	1030 ± 10	67.4 ± 0.1	7.51 ± 0.07
	51	5.71 ± 0.12	1011 ± 7	72.3 ± 0.7	8.21 ± 0.05
	9.5	1.09 ± 0.03	955 ± 5	77.1 ± 0.7	8.47 ± 0.23
5.6 + 5	100	13.44 ± 0.02	1017 ± 5	68.6 ± 0.2	9.37 ± 0.21
	51	7.07 ± 0.01	997 ± 3	73.6 ± 0.1	10.18 ± 0.16
	9.5	1.32 ± 0.01	936 ± 2	76.0 ± 0.1	9.88 ± 0.07
4.0 + 4.5 with PProDOT	100	13.08 ± 0.03	999 ± 3	75.2 ± 3	9.90 ± 0.38
	51	7.00 ± 0.13	981 ± 6	77.1 ± 3	10.36 ± 0.52
	9.5	1.32 ± 0.04	919 ± 6	79.2 ± 3	10.11 ± 0.62

Supplementary Table S3. The charge transfer resistance (R_{CT}) at the counter electrode. Two similar electrodes with the electrolyte at a given distance 65 μm between them leaving 0.6 x 0.6 cm^2 are assembled and electrochemical impedance spectroscopy (EIS) under dark conditions was performed at 0V in a frequency range between 1 MHz and 0.1 Hz in 50mV steps. The diffusion coefficient of $[Co(bpy\text{-}pz)_2]^{3+/2+}$ redox system determined from this measurement were between $2 \cdot 10^{-6}$ to $4 \cdot 10^{-6}$ cm^2/s.

Redox	Pt	PProDOT
$[Co(bpy\text{-}pz)_2]^{3+/2+}$	~50	~2.5
I_3^-/I^-	~0.8	-